HHS Public Access

Author manuscript

Gastroenterology. Author manuscript; available in PMC 2020 March 01.

Published in final edited form as:

Gastroenterology. 2019 March ; 156(4): 1066–1081.e16. doi:10.1053/j.gastro.2018.11.024.

BHLHA15-positive Secretory Precursor Cells Can Give Rise to Tumors in Intestine and Colon in Mice

Yoku Hayakawa[1,2,8,*], **Mayo Tsuboi**[1,8], **Samuel Asfaha**[3], **Hiroto Kinoshita**[1], **Ryota Niikura**[1], **Mitsuru Konishi**[1], **Masahiro Hata**[1], **Yukiko Oya**[1], **Woosook Kim**[2], **Moritz Middelhoff**[2], **Yohko Hikiba**[4], **Naoko Higashijima**[4], **Sozaburo Ihara**[4], **Tetsuo Ushiku**[5], **Masashi Fukayama**[5], **Yagnesh Tailor**[2], **Yoshihiro Hirata**[1], **Chandan Guha**[6], **Kelley S. Yan**[2,7], **Kazuhiko Koike**[1], and **Timothy C. Wang**[2,*]

[1]Department of Gastroenterology, Graduate school of Medicine, the University of Tokyo, Tokyo, 1138655, Japan

[2]Division of Digestive and Liver Disease, Department of Medicine,Columbia University, New York, NY, 10032, USA

[3]Department of Medicine, University of Western Ontario, London, ON N6A 5W9, Canada

[4]The Institute for Adult Diseases, Asahi-life Foundation, Tokyo, 103-0002, Japan

[5]Department of Pathology, Graduate school of Medicine, the University of Tokyo, Tokyo, 1138655, Japan

[6]Department of Radiation Oncology, Albert Einstein College of Medicine, NY, 10467, USA

[7]Department of Genetics and Development, Columbia University, New York, NY, 10032, USA

[8]Co-first authors

Abstract

Background & Aims: The intestinal epithelium is maintained by long-lived intestinal stem cells (ISCs) that reside near the crypt base. Above the ISC zone, there are short-lived progenitors that normally give rise to lineage-specific differentiated cell types but can dedifferentiate into ISCs in

[*]**Corresponding Authors:** Timothy C. Wang, M.D., Chief, Division of Digestive and Liver Diseases, Silberberg Professor of Medicine, Department of Medicine and Irving Cancer Research Center, Columbia University Medical Center, 1130 St. Nicholas Avenue, Room #925, New York, NY 10032-3802, USA, Tel: 212-851-4581, Fax: 212-851-4590, tcw21@cumc.columbia.edu; Yoku Hayakawa, M.D., Ph.D., Assistant Professor, Department of Gastroenterology, Graduate School of Medicine, The University of Tokyo, 7-3-1, Hongo, Bunkyo-ku, Tokyo, 1138655, Japan, Tel: 81-3-3815-5411, Fax: 81-3-5800-8812, yhayakawa-tky@umin.ac.jp.

Author contributions:

Y.Hayakawa and T.C.W. contributed to the study supervision and coordination, and the design of the experiments. Y.Hayakawa & M.T. conducted and performed all experiments. S.A., H.K., M.K., M.H., W.K., M.M., Y.Hikiba, N.H., S.I., Y.T., Y.Hirata, C.G. assisted various portions of the experiments and analysis of data. Y.Hayakawa and R.N. analyzed the data of human samples. T.U. and M.F. assisted pathological diagnosis. Y.Hayakawa., S.A., Y.Hirata, K.S.Y., K.K., and T.C.W. wrote the manuscript.

Disclosures:

The authors disclose no conflicts.

Transcript profiling:

GSE111934.

certain circumstances. However, the role of epithelial dedifferentiation in cancer development has not been fully elucidated.

Methods: We performed studies with *Bhlha15*-CreERT, *Lgr5*-DTR-GFP, *Apc*$^{flox/flox}$, LSL-Notch (IC), and R26-reporter strains of mice. Some mice were given diphtheria toxin to ablate *Lgr5* mRNA-positive cells, irradiated, or given 5-fluorouracil, hydroxyurea, doxorubicin, or dextran sodium sulfate to induce intestinal or colonic tissue injury. In intestinal tissues we analyzed the fate of progeny that expressed *Bhlha15* mRNA. We used microarrays and reverse-transcription PCR to analyze gene expression patterns in healthy and injured intestinal tissues and in tumors. We analyzed gene expression patterns in human colorectal tumors using the TCGA dataset.

Results: *Bhlha15* identified Paneth cells and short-lived secretory precursors (including pre-Paneth label-retaining cells) located just above the ISC zone in the intestinal epithelium. *Bhlha15*+ cells had no plasticity after loss of *Lgr5*-positive cells or irradiation. However, *Bhlha15*+ secretory precursors started to supply the enterocyte lineage after doxorubicin-induced epithelial injury in a Notch-dependent manner. Sustained activation of Notch converts *Bhlha15*+ secretory precursors to long-lived enterocyte progenitors (EPs). Administration of doxorubicin and expression of an activated form of Notch resulted in a gene expression pattern associated with EPs, whereas only sustained activation of Notch altered gene expression patterns in *Bhlha15*+ precursors, towards that of ISCs. *Bhlha15*+ EPs with sustained activation of Notch formed intestinal tumors with serrated features in mice with disruption of *Apc*. In the colon, *Bhlha15* marked secretory precursors that became stem-like, cancer-initiating cells following dextran sodium sulfate-induced injury, via activation of Src and YAP signaling. In analyses of human colorectal tumors, we associated activation of Notch with chromosome instability-type tumors with serrated features in the left colon.

Conclusion: In mice, we found that short-lived precursors can undergo permanent reprogramming by activation of Notch and YAP signaling. These cells could mediate tumor formation, in addition to traditional ISCs.

Keywords

tumorigenesis; interconversion; colon cancer; Yes associated protein 1

Introduction

The intestinal epithelium is highly proliferative and rapidly turns over every 4–5 days[1]. Epithelial turnover is maintained by long-lived self-renewing intestinal stem cells (ISCs) that reside near the crypt base. ISCs divide continuously to give rise to their multi-lineage progeny throughout the crypt-villus unit. In the hierarchical model of intestinal epithelial cells, ISCs first produce the lineage-committed short-lived progenitors within the transit-amplifying (TA) cell zone, that after several cell divisions become committed to either the secretory or enterocyte lineage[1]. The secretory lineage includes goblet cells, enteroendocrine cells, and Paneth cells. Epithelial tuft cells are also presumed to be part of the secretory lineage, however, there remains some debate as to whether they are derived directly from either secretory or enterocyte progenitors, or generated from an independent precursor[2].

Notch, Wnt, and Rspo signaling are critical for determining ISC cell fate and homeostasis[3, 4]. Wnt activation in ISCs enhances differentiation into the secretory cell lineage, while Notch activation in ISCs directs enterocyte differentiation with loss of the secretory lineage[3, 5]. Multiple markers of ISCs and progenitors have been described to date. *Lgr5* is expressed in actively cycling crypt base columnar (CBC) cells distributed between Paneth cells[6]. In addition, there appears to be a distinct ISC pool near the "+4" position, just above *Lgr5*$^{+}$ CBC cells, which comprises more quiescent ISCs. Interestingly, recent transcriptome analyses revealed that *Bmi1*-expressing cells also comprise a subset of enteroendocrine cells, which have been shown to interconvert to actively cycling ISCs in order to maintain epithelial homeostasis following acute injury[7–12]. Similarly, several short-lived progenitors and pre-Paneth label-retaining cells (LRCs) that express low levels of *Lgr5*, can also participate in the interconversion process through dedifferentiation, particularly when *Lgr5*$^{+}$ ISCs are damaged[13–15]. It has been thought that such progenitors phenotypically and genetically dedifferentiate to *Lgr5*$^{+}$ ISCs, and then contribute to regeneration[11, 12].

ISCs are considered to be the primary cellular origin of intestinal tumors due to their longevity and self-renewing capacity. This is supported by mouse models, where oncogenic mutations in ISCs result in efficient dysplasia formation, whereas similar mutations in more differentiated cells fail to produce dysplasia[16]. To date, there is limited evidence that even short-lived progenitors can be a source of intestinal cancers, despite their potential to de-differentiate. Indeed, differentiated post-mitotic cells with genetic mutations can give rise to cancers in rare circumstances, such as in the presence of inflammation or aberrant NF-κB activation[17, 18]. We have recently reported that gastric stem cells expressing *Bhlha15* (also known as *Mist1*), a basic helix-loop-helix transcriptional factor, can give rise to cancers[19–22]. Here, we report the presence of *Bhlha15* expression in both the small intestinal and colonic epithelium, and investigate the identity and function of these cells.

Methods

Mice

Bhlha15-CreERT and *Eef1a1*-LSL-*Notch1(IC)* mice[19] were described previously. LSL-*Kras*^{G12D} and LSL-*Trp53*^{R172H} mice were provided by Dr. Kenneth Olive (Columbia University). *Apc*^{flox} and *Lgr5*-DTR-GFP mice were obtained from the National Cancer Institute and Genentech, respectively. *R26* reporter mice were purchased from the Jackson Laboratory. Cre recombinase was activated by oral administration of TAM (2mg/0.2mL corn oil). Mouse and in vitro culture experiments were repeated at least 2 times, with at least 3 biological replicates, and representative results are shown. All animal studies and procedures were approved by the ethics committees at Columbia University and the University of Tokyo.

Treatment

To induce epithelial injury, hydroxyurea, 5-fluorouracil, and doxorubicin (Sigma) were administered intraperitoneally at a dose of 1g/kg, 150mg/kg, and 15mg/kg, respectively. To induce colonic injury, 2% dextran sodium sulfate (DSS) was given for 5 days. For *Lgr5*$^{+}$ cell

ablation, DT was administered via intraperitoneal injection at a dose of 50ug/kg. Whole body irradiation at a dose of 10 or 12 Gy was given to some mice. Src inhibitor (Saracatinib, Caymanchemicals) and γ-secretase inhibitor dibenzazepine (DBZ, Tocris BioScience) were administered at indicated time points orally at a dose of 50mg/kg and intraperitonially at a dose of 5 mg/kg, respectively. Bone marrow transplantation and EdU label retention assay was performed as described previously[23, 24].

More detailed information is described in Supplementary Methods.

Results

Bhlha15 is expressed in short-lived secretory precursors in the small intestine

We performed lineage tracing experiments using *Bhlha15*-CreERT; *R26*-mTmG mice. We observed recombined GFP$^+$ Paneth cells (at the crypt base below the +4 position) immediately following tamoxifen induction (Fig. 1A). We also detected another GFP$^+$ cell population situated between positions +5 and +10 that was morphologically distinct from Paneth cells (Fig. 1B). We confirmed using an antibody that recognizes estrogen receptor that CreERT protein is expressed at the same locations, but was not expressed in the villus compartment (Fig. S1A). Analogous to this expression pattern, *in situ* hybridization and immunohistochemistry revealed that *Bhlha15* mRNA and protein are strongly expressed in Paneth cells, and is moderately expressed in the TA cell zone (Fig. S1A). From day 1 to 5 after tamoxifen induction, there was an increase in the number of recombined non-Paneth cells that rapidly migrate upwards in the villus-crypt units, but these cells disappeared in around 10 days (Fig. 1A&S1B). Recombined Paneth cells persisted longer, but eventually turned over and disappeared after 90 days. This short-term supply for scattered cells appears to be similar to that reported in *Dll1*-CreERT mice[13], which labels short-lived secretory progenitors. Indeed, cells in the *Bhlha15* lineage include chromogranin A or synaptophysin-positive enteroendocrine cells, DCLK1$^+$ tuft cells, MUC2$^+$ goblet cells, and Lysozyme$^+$ Paneth cells, but not FABP1$^+$ enterocytes (Fig. 1C). More specifically, TdTomato expression is found predominantly in Paneth cells at the earliest time point, while a subset of TA and a few goblet cells are also labeled in the TA cell zone and lower villus (Fig. S1B). At 4 days after tamoxifen, the TdTomato$^+$ population contains a greater proportion of goblet cells and newly includes tuft and enteroendocrine cells. However, most of these labeled cells, except for Paneth cells, rapidly disappear by day 7, suggesting that *Bhlha15* marks secretory precursors that can supply goblet, enteroendocrine, and tuft cell lineages only for the short-term, as well as relatively long-lived Paneth cells.

Next, we compared the expression of the ISC marker *Lgr5* to *Bhlha15*$^+$ cells in *Bhlha15*-CreERT; *Lgr5*-DTR-EGFP; *R26*-TdTomato mice[9]. Based on FACS and histological analysis, we found no strong *Lgr5*-GFP expression in intestinal *Bhlha15*$^+$ cells; only a subset of *Bhlha15*$^+$ cells expressed low levels of *Lgr5*-GFP, which suggests that *Bhlha15*$^+$ cells may contain the previously described *Lgr5*-expressing, pre-Paneth LRCs[15, 24] (Fig. 1D–F&S1C). Indeed, when using the EdU label retention protocol, we found that 73% of LRCs express *Bhlha15* (Fig. S1D–E). However, since we did not observe sustained, confluent lineage tracing, these *Lgr5*-expressing *Bhlha15*$^+$ cells are likely distinct from *Lgr5*$^+$ ISCs.

Transcriptome analysis of *Bhlha15*-expressing populations in the small intestine.

Bhlha15-expressing TdTomato^{+} cells isolated from induced *Bhlha15*-CreERT; *R26*-TdTomato mice can be divided into three distinct populations: CD24^{neg}, CD24^{lo}, and CD24^{hi} (Fig. 2A). *Bhlha15*$^{+}$*Lgr5*^{lo} pre-Paneth precursors belong to the CD24^{hi} population, together with *Bhlha15*$^{+}$*Lgr5*^{neg} mature Paneth cells (Fig. S1F–G). We isolated CD24^{lo} and CD24^{hi} populations by FACS, and performed gene expression analysis. Principal components analysis (PCA) of the microarray data showed that *Bhlha15*$^{+}$CD24^{lo} and *Bhlha15*$^{+}$CD24^{hi} cells are molecularly distinct populations (Fig. 2B). Hierarchical clustering indicated that *Bhlha15*$^{+}$CD24^{hi} cells express high levels of Paneth cell-specific genes, including defensin family genes, *Lyz1*, and *Mmp7*, suggesting Paneth cell enrichment (Fig. 2C). *Bhlha15*$^{+}$CD24^{hi} cells also highly express Wnt-target genes such as *Sox9* or *Axin2*, and even stem cell marker genes including *Lgr5, Troy, Hopx*, and *Ascl2*. GSEA analysis also suggested that ISC-related genes are enriched in CD24^{hi} population compared to CD24^{lo} population (Fig. 2D). In addition, genes associated with LRCs, such as *Mex3a*, *Cd83*, and *Nfat5*[15, 24], are enriched in *Bhlha15*$^{+}$CD24^{hi} cells, confirming that *Bhlha15*$^{+}$CD24^{hi} cells contain pre-Paneth LRCs (Fig. 2C–D). In contrast, proliferation marker genes including the cyclin family and *Mki67* as well as markers of TA progenitors such as *Dll1, Tert, Krt19*, and *Alpi*, are more prominently expressed in *Bhlha15*$^{+}$CD24^{lo} cells, suggesting that *Bhlha15*$^{+}$CD24^{lo} cells may represent a secretory precursor population.

RT-PCR analysis of these cells validated the microarray results (Fig. 2E). Although *Reg4*, a secretory progenitor marker[25], appears to be predominantly expressed in *Bhlha15*$^{+}$CD24^{hi} cells, *Bhlha15*$^{+}$CD24^{lo} cells showed prominent expression of *Tac1*, consistent with the labeling of secretory precursors as reported[5, 25]. Analysis of *Atoh1*-GFP mice and TAC1 immunofluorescence revealed that *Atoh1* is expressed in both populations, while *Tac1* is specifically expressed in secretory progenitors (Fig. 2E–F). *Dll1* expression was not significantly different between CD24^{lo} and CD24^{hi} populations, and we found using immunohistochemistry and in situ hybridization that the vast majority of *Bhlha15*$^{+}$ cells did not express DLL1 (Fig. 2E–F&S2A–C). In fact, GSEA analysis showed that genes enriched in reported *Dll1*$^{+}$ progenitors[13] are not necessarily upregulated in *Bhlha15*$^{+}$CD24^{lo} cells (Fig. 2D), suggesting that while *Dll1*$^{+}$ and *Bhlha15*$^{+}$ progenitors exhibit some similarities, they are highly likely to be distinct populations. On the other hand, cyclin D1, CDX2, KRT7, and Ki67 are expressed mostly in *Bhlha15*$^{+}$ secretory precursors rather than mature Paneth cells at the crypt base, while SOX9 is mainly expressed in Paneth cells but not in secretory precursors (Fig. 2F&S2D). Proliferation rates in TdTomato^{+} cells in the TA cell zone rapidly decreased by day 4, suggesting that the majority of initially labeled *Bhlha15*$^{+}$ secretory precursors quickly generate progeny and turn over by this time point (Fig. S2E). It should be noted that approximately 30% of Ki67^{+}TdTomato^{+} cells express MUC2, likely representing immature pre-goblet cells (Fig. S2F). Together, *Bhlha15*-expressing TA cells mark a short-lived secretory precursor population, which might include a subset of lineage-committed pre-goblet cells.

Bhlha15$^+$ precursors are chemo-radioresistant, but do not convert to long-lived ISCs following injury

Dll1$^+$ progenitors can revert to stem-like cells following irradiation-induced injury[13]. To test whether this is also true of *Bhlha15*$^+$ precursors, we irradiated the *Bhlha15*-CreERT; *R26*-TdTomato mice and examined the subsequent cell fate mapping at various time intervals (Fig. 3A). When using a sensitive *R26*-TdTomato mouse line, we found quite rare stem cell-type lineage tracing, with labeling of the entire villus-crypt unit from the *Bhlha15*-lineage, but >99% of glands show secretory specific labeling as seen in crossed to the *R26*-mTmG line. Following 10 Gy irradiation, recombination occurs as the same pattern as in the unirradiated state without any apoptosis in *Bhlha15*$^+$ cells, but there was no significant increase in stem cell-type lineage tracing events, suggesting that irradiation does not rigorously induce interconversion of *Bhlha15*$^+$ lineage as was reported for *Dll1*$^+$ cells (Fig. 3B&E, S3A). Given that ablation of *Lgr5*$^+$ stem cells can alter the fate and induce lineage tracing from some facultative progenitors, we then treated *Bhlha15*-CreERT; *Lgr5*-DTR-EGFP; *R26*-TdTomato mice with diphtheria toxin (DT) in order to ablate *Lgr5*$^+$ cells. Following *Lgr5*$^+$ cell ablation, we observed no remarkable change in the *Bhlha15*$^+$ cell recombination pattern above TA cell zone, while there was a dramatic decrease in labeled Paneth cell numbers. (Fig. 3B&E, S3B). Thus, while *Bhlha15*$^+$ precursors can survive and supply secretory progeny following irradiation and *Lgr5*-DT induced injury, they do not interconvert into stem-like cells, indicating that *Bhlha15*$^+$ cells are functionally distinct from other reserve stem cell populations, such as those expressing *Dll1, Alpi*, or *Bmi1*.

It was also reported that cytotoxic agents can through cellular injury induce the dedifferentiation of pre-Paneth LRCs into stem-like cells[15]. While we observed no evidence of stem cell conversion following 5-fluorouracil or hydroxyurea treatment (not shown), lineage expansion and stem-like tracing from *Bhlha15*$^+$ cells were observed following doxorubicin treatment (Fig. 3B). Given that proliferation was observed in Lysozyme$^-$ progenitors but not in Lysozyme$^+$ mature Paneth cells after doxorubicin treatment (Fig. 3C–D), these clones are likely derived from the more undifferentiated precursor population rather than mature Paneth cells.

Nevertheless, after complete epithelial regeneration at 20–30 days post injury, lineage tracing events from *Bhlha15*$^+$ cells gradually disappeared and only a few Paneth cells remained traced by the TdTomato reporter (Fig. 3B–E). Thus, *Bhlha15*$^+$ progenitors can transiently contribute to crypt regeneration following doxorubicin-induced injury, but quickly lose this capacity and cease expanding, perhaps due to contributions from other stem or progenitor cells. Moreover, during transient lineage tracing from doxorubicin-treated *Bhlha15*$^+$ cells, *Bhlha15*-derived clones contain FABP1$^+$ enterocytes which are not normally derived from *Bhlha15*$^+$ secretory precursors (Fig. 3F). On the other hand, the numbers of secretory cells such as enteroendocrine, goblet cells, and Paneth cells are decreased in the doxorubicin-treated *Bhlha15*$^+$ lineage, suggesting that *Bhlha15*$^+$ secretory precursors interconvert to short-lived enterocyte progenitors (EPs) and cease to supply secretory cells after doxorubicin-induced injury.

Bhlha15$^+$ precursors show long-term enterocyte-specific lineage tracing with sustained Notch activation

Notch signaling regulates intestinal epithelial cell differentiation by controlling stem cell fate. Indeed, a Notch downstream molecule HES1 is upregulated in *Bhlha15*$^+$ precursor cells rather than in Paneth cells after doxorubicin treatment, whilst HES1 is not expressed in these cells in normal, irradiated, or *Lgr5*-ablated intestines (Fig. S3C). Cells in *Bhlha15*-derived clones are strongly positive for HES1 one week after doxorubicin treatment (Fig. S3D), suggesting that the Notch pathway in *Bhlha15*$^+$ precursors is specifically activated by doxorubicin and contributes to regeneration. Therefore, we examined the effect of Notch activation in *Bhlha15*$^+$ secretory precursors by generating *Bhlha15*-CreERT; LSL-Notch(IC) mice that enabled us to conditionally activate the Notch pathway in *Bhlha15*$^+$ cells. After Notch activation, recombined *Bhlha15*$^+$ cells initially showed strong HES1 expression in both precursor and Paneth populations, and later expanded and produced completely traced crypt-villus units that were long-lived (greater than 180 days), in contrast to normal *Bhlha15* progeny that were restricted only to Paneth cells at later time points (Fig. 4A&S3C–E). Multicolor labeling of the *Bhlha15* lineage using *R26*-Confetti mice revealed multicolor Paneth cells in the normal state, whereas single-color, monoclonal expansion of *Bhlha15* lineage was seen with NICD expression (Fig. 4B). In organoid culture, the addition of Wnt3A to standard culture media containing EGF, Noggin and R-spondin1 (WENR) failed to induce expansion of the recombined *Bhlha15* lineage, although we did observe GFP$^+$ Paneth cells at sites of budding crypts (Fig. 4C&S3F–G). In contrast, addition of the Notch ligand Jagged-1 to culture (JENR) or induction of Notch(IC) expression induced lineage tracing from *Bhlha15*$^+$ cells.

At 5 days after tamoxifen induction, we observed in *Bhlha15*-CreERT; *R26*-TdTomato; LSL-Notch(IC) murine crypts the beginning of red ribbon tracing from the +5 to +10 region, whereas Lysozyme$^+$TdTomato$^+$ Paneth cells did not show such clonal expansion at the crypt base (Fig. 4D). Proliferation was observed in Lysozyme$^-$ progenitors but not in Lysozyme$^+$ mature Paneth cells (Fig. 4E). Moreover, traced TdTomato$^+$ glands expressed CDX2, which is normally not expressed in the mature Paneth cell population (Fig. 4D). Thus, aberrant Notch activation in secretory precursors, rather than in mature Paneth cells, converts cells into stem-like cells. Nevertheless, we observed a complete loss of secretory cells including goblet, Paneth, enteroendocrine, and tuft cells in Notch-activated *Bhlha15* lineage, and such villus-crypt units are completely replaced by the FABP1$^+$ enterocyte lineage (Fig. 4F&3E). Thus, in the setting of Notch activation, *Bhlha15*$^+$ secretory precursors interconvert into unipotent enterocyte progenitors, similar to what is observed following treatment with doxorubicin, although interconversion appears to be long-lived when sustained Notch activation is present. To confirm that Notch pathway is critical for doxorubicin-induced interconversion, we treated mice with DBZ, a Notch inhibitor. DBZ treatment significantly decreased *Bhlha15*-derived tracing events following doxorubicin, supporting the importance of Notch pathway in this process (Fig. S3H). In contrast to what is seen with *Bhlha15*-CreERT mice, NICD expression did not alter the frequency of lineage tracing in *Lgr5*-CreERT and *Dclk1*-CreERT mice (Fig. S4A–C), suggesting that Notch signaling does not convert all intestinal epithelial cells into more active progenitors, and that the tracing ability

of *Lgr5*$^{+}$ cells is not enhanced by additional forced Notch activation, which is not surprising given the constitutive Notch-active status in *Lgr5*$^{+}$ cells.

Distinct gene profiles in activated *Bhlha15*$^{+}$ precursors.

We performed transcriptome analysis of injury-treated and Notch-activated *Bhlha15*$^{+}$ cell populations, as well as *Lgr5*^{hi} ISCs. PCA analysis revealed that *Lgr5*-DT ablation induces minimal changes in both CD24^{lo} and CD24^{hi} populations, while irradiation and doxorubucin treatment induce more prominent changes (Fig. 5A). Following NICD expression, dramatic shifts of gene expression can be found in both CD24^{lo} and CD24^{hi} cells, while they nevertheless retain their clear and distinct gene signatures. NICD-expressing *Bhlha15*$^{+}$ cells and *Lgr5*^{hi} ISCs still display clearly distinct gene signatures, although both cell lineages appear to show longevity and tracing ability in mice. Hierarchical clustering supports these findings, demonstrating that irradiation and doxorubicin treatments induce similar gene alterations while changes in doxorubicin treatments are broader, and NICD expression produces a quite different pattern of transcriptional activation (Fig. S5A–B).

When compared with untreated CD24^{lo} and CD24^{hi} populations, the NICD-expressing CD24^{lo} population exhibits an upregulation of stem cell-related markers such as *Lgr5*, *Cd44*, *Troy*, or *Axin2*, while the NICD^{+}CD24^{hi} population shows only mild upregulation of *Lgr5* (Fig. 5B). Such upregulation of stem cell markers is not obvious in cells treated with *Lgr5*-DT, irradiation, or doxorubicin. GSEA curves suggest that irradiation and doxorubicin treatments are in fact negatively associated with ISC gene signatures in both CD24^{lo} and CD24^{hi} cells, while NICD expression shows a significant positive association with ISC markers only in CD24^{lo} cells (Fig. 5C&S4C). Colony formation ability was predominantly limited to *Bhlha15*$^{+}$CD24^{lo} secretory precursors in which NICD expression was induced, compared to *Bhlha15*$^{+}$CD24^{hi} cells or cells sorted from injury models (Fig. 5D). Thus, short-term expansion induced by doxorubicin may not represent true stem cell interconversion either phenotypically or genetically, while Notch activation might induce permanent reprogramming in CD24^{lo} secretory progenitors but not in CD24^{hi} Paneth and pre-Paneth LRCs. Nevertheless, it should be noted that the “shift” towards ISC gene signature in *Bhlha15*$^{+}$CD24^{hi} cells likely represents the acquisition of only a few ISC properties, given the clearly distinct gene expression pattern from *Lgr5*^{hi} ISCs, and this is likely due to the limited differentiation ability of *Bhlha15*$^{+}$NICD^{+} clones, in contrast to the multipotency in ISCs.

At one month after tamoxifen treatment, we detected *Lgr5*-expressing CBCs that were derived from Notch-activated *Bhlha15*$^{+}$Tomato^{+} clones (Fig. 5E&S5F), suggesting that *Bhlha15*$^{+}$NICD^{+} cells are able to convert to *Lgr5*$^{+}$ cells, consistent with our transcriptome analysis. Nevertheless, multiple DT treatments, resulting in complete ablation of *Lgr5*$^{+}$ cells and even Paneth cell lineage[10], did not diminish the lineage tracing ability of *Bhlha15*$^{+}$NICD^{+} cells (Fig. 5F), suggesting that *Lgr5*$^{+}$ cell populations may be dispensable for the initiation and maintenance of *Bhlha15*$^{+}$ clones even following Notch activation.

Genes enriched in enterocyte progenitors (EPs), such as *Sox4*26, *Afp* and *Snap25*[11], are upregulated in both NICD-expressing CD24^{lo} and CD24^{hi} cells (Fig. 5B), consistent with the phenotypic conversion from secretory precursors to EPs by sustained Notch activation.

Moreover, the enterocyte markers *Alpi*, *Fabp1, Apoa1, or Apoa4*26 were upregulated in doxorubicin-treated CD24^{lo} and CD24^{hi} cells. Upon GSEA analysis, doxorubicin-treated CD24^{hi} cells, NICD^{+}CD24^{lo} cells, and NICD^{+}CD24^{hi} cells all showed significant gene enrichment with EP gene signatures, although doxorubicin-treated CD24^{lo} cells and cells from irradiated or *Lgr5*-ablated mice did not (Fig. 5C&S5C). Treatment with doxorubicin during EdU pulse administration increased label retention efficiency in *Bhlha15*$^{+}$ cells (Fig. S1D–E), suggesting CD24^{hi} pre-Paneth LRCs may contribute to doxorubicin-induced enterocyte clones in a greater extent than CD24^{lo} precursors.

In fact, we observe gradual decrease and complete disappearance of *Lgr5* expression by day 7 in the doxorubicin-treated *Lgr5*-CreERT-IRES-EGFP mice (Fig. S5D). Nevertheless, there are equivalent numbers of lineage tracing from *Lgr5*$^{+}$ cells after doxorubicin treatment compared to untreated mice, likely produced by surviving *Lgr5*$^{+}$ CBCs and interconverted *Lgr5*$^{+}$ LRCs. *Lgr5* ablation indeed increased the lineage tracing events from *Bhlha15*$^{+}$ cells when combined with doxorubicin treatment (Fig. S5E). Thus, while *Bhlha15*$^{+}$ secretory precursors normally do not show tracing events following *Lgr5* ablation, once they give rise to EPs following doxorubicin, these cells readily respond to *Lgr5* ablation to supply cryptic cells.

NICD^{+}*Bhlha15*$^{+}$ precursors contribute to regeneration and cancer.

Given that *Bhlha15*$^{+}$ precursors are radioresistant, we investigated whether Notch activation in *Bhlha15*$^{+}$ progenitors may contribute to epithelial regeneration following lethal 12Gy whole body irradiation (Fig. 6A). *Bhlha15*-CreERT; LSL-Notch(IC); *R26*-TdTomato mice demonstrated abundant, fully lineage-traced intestinal glands, indicating that Notch-activated *Bhlha15*$^{+}$ cells contribute to the maintenance of intestinal crypt-villus units (Fig. 6A). Accordingly, *Bhlha15*-CreERT; LSL-Notch(IC) mice display significantly longer survival than control mice (Fig. 6B).

Next, we analyzed the tumorigenic potential in *Bhlha15*$^{+}$ cells in the intestine. We generated *Bhlha15*-CreERT; *Apc*$^{flox/flox}$ mice for conditional deletion of *Apc* in *Bhlha15*$^{+}$ cells. Previous studies have shown that *Apc* loss in fast dividing *Lgr5*$^{+}$ and *Krt19*$^{+}$ stem cells leads to intestinal tumors and acute lethality[7, 16]. However, *Apc* loss in *Bhlha15*$^{+}$ cells alone did not result in the spontaneous development of intestinal tumors nor acute lethality (Fig. 6C–D). Even when mice were treated with irradiation or doxorubicin, these mice did not develop tumors nor dysplasia (Fig. S6A). Thus, secretory precursors and differentiated secretory cells do not act as an origin of intestinal tumors in these settings. However, when *Bhlha15*-CreERT; *Apc*$^{flox/flox}$ mice were crossed to LSL-Notch(IC) mice, they rapidly developed intestinal tumors resulting in death within 6 weeks (Fig. 6C–D&S6B). These tumors show strong HES1 expression with serrated histological features, both of which are not evident in intestinal tumors in *Lgr5*-CreERT; *Apc*$^{flox/flox}$ mice (Fig. S6B–C). Simultaneous induction of mutant *Kras*^{G12D} or *Trp53*^{R172H} in the NICD^{+}*Bhlha15* lineage led to serrated-type hyperplasia (Fig. S6D). In contrast, simultaneous expression of mutant *Kras*^{G12D} or *Trp53*^{R172H} without Notch activation did not induce tumor formation even with loss of Apc. Thus, accumulation of multiple classical oncogenic mutations is not sufficient for the conversion from secretory progenitors into cancer-initiating cells, while activation of the

Notch pathway is uniquely able to induce serrated-type malignant transformation through conversion to enterocyte lineage.

The tumors observed in *Bhlha15*-CreERT; LSL-Notch(IC); $Apc^{flox/flox}$ mice showed strong Ki67 positivity and nuclear translocation of β-catenin (Fig. 6E–F). Although nuclear β-catenin staining could be found both in Lysozyme$^+$ mature Paneth cells and dysplastic cells in *Bhlha15*-CreERT; LSL-Notch(IC); $Apc^{flox/flox}$ mice, Ki67$^+$ proliferation was restricted in dysplastic cells and was not evident in mature Paneth cells (Fig. 6F). In addition, the presence of abundant CDX2 expression and the absence of Lysozyme expression points to undifferentiated secretory precursors rather than mature Paneth cells, as the probable initial source of these tumors.

Bhlha15 marks colonic secretory precursors that can convert to stem-like, tumor-initiating cells following injury.

Next, we investigated the characters of *Bhlha15*$^+$ cells in the colon. Tamoxifen induction of *Bhlha15*-CreERT; *R26*-mTmG mice revealed that *Bhlha15*$^+$ cells were initially found at the +1 to +10 position with the peak at +4 or +5 near the colonic gland base (Fig. 7A&S7A). *In situ* hybridization and immunohistochemistry confirmed the endogenous expression pattern for this marker in the colon (Fig. S7B–C). Upon FACS analysis, the colonic *Bhlha15*$^+$ cells overlapped with CD24$^+$ cells (Fig. 7B). RT-PCR results from sorted *Bhlha15*$^+$CD24$^+$ cells revealed that these cells expressed high levels of *Bhlha15* as well as *Atoh1* (Fig. 7C). Furthermore, *Bhlha15*$^+$CD24$^+$ cells expressed high levels of *Ckit* and *Reg4*, which have been recently identified as colonic deep crypt secretory cell markers[27, 28]. However, *Lgr5* was not highly expressed in *Bhlha15*$^+$CD24$^+$ cells, and *ChgA* expression was highest in *Bhlha15*$^-$CD24$^+$ cells that appeared to contain differentiated enteroendocrine cells.

Around 5 days after tamoxifen induction, there was an increase in the number of *Bhlha15*-derived GFP$^+$ cells in the colonic glands, indicating that *Bhlha15*$^+$ colonic cells rapidly generate progeny (Fig. 7A). These progenies contained MUC2$^+$ goblet cells and DCLK1$^+$ tuft cells, but not carbonic anhydrase 2$^+$ absorptive cells, and almost all *Bhlha15*$^+$-derived cells disappeared after 15 days, suggesting that *Bhlha15*$^+$ colonic cells include short-lived secretory precursors (Fig. S7E).

We observed that the *Bhlha15*$^+$ cells and *Lgr5*$^+$ cells were located in close proximity but were nevertheless mostly distinct lineages in the colonic sections, although FACS analysis did show rare (9.93% in *Lgr5*$^+$ cells) overlap (Fig. 7B&S7D). We found rare fully traced glands from *Bhlha15*$^+$ cells even in normal homeostasis, suggesting that *Bhlha15*$^+$ cells may occasionally overlap with the colonic stem cell population (Fig. S8A–B). However, we observed no apparent changes in lineage tracing pattern even after *Lgr5* ablation (Fig. S7D&S8B). Analogous to the intestine, Notch activation in *Bhlha15*$^+$ cells led to loss of the secretory lineage and a shift to absorptive lineage tracing (Fig. S7E). Nevertheless, the increase in *Bhlha15*-derived gland tracing events was not statistically significant, even with combined *Lgr5* ablation (Fig. S8B), suggesting that interconversion is not efficiently induced by Notch activation in the colon. In contrast, dextran sodium sulfate (DSS)-induced injury significantly increased the lineage tracing ability in *Bhlha15*$^+$ cells, while most of *Lgr5*$^+$ cells disappeared (Fig. S8A–C).

Unlike doxorubicin-treated small intestinal *Bhlha15*$^{+}$ cells, *Bhlha15*$^{+}$ colonic precursors did not show HES1 expression even after DSS treatment (Fig. S8D). Recently, it has been recognized that the YAP/TAZ-mediated mechanosensory pathway plays a central role in colonic regeneration after DSS treatment[29]. Indeed, we found upregulation of YAP expression in regenerative glands after DSS, in which *Bhlha15*$^{+}$ cells become positive for YAP, while no such upregulation following *Lgr5*-DTR ablation or forced Notch activation (Fig. 7D&S8E–F). Since YAP coordinates Wnt activity as a transcriptional coactivator, we examined Wnt signaling status in the sorted *Bhlha15*$^{+}$ cells with or without DSS treatment. RT-PCR and immunohistochemical analysis revealed that DSS-treated *Bhlha15*$^{+}$ cells showed upregulation of Wnt target molecules, including *Lgr5, Olfm4, Cd44, Axin2*, and cyclin D1, compared to normal *Bhlha15*$^{+}$ cells (Fig. 7D&S8F–G). Following DSS treatment, we observed nuclear translocation of beta-catenin in cells in regenerative glands, including *Bhlha15*$^{+}$ cells (Fig. S8H). We also found increased colony formation ability of *Bhlha15*$^{+}$ cells following DSS treatment (Fig. S8I). Thus, DSS treatment leads to greater Wnt activation in *Bhlha15*$^{+}$ cells, which likely contributes to greater stem cell potential. After DSS treatment, *Bhlha15*$^{+}$ cells also start to express phosphorylated Src that activates YAP pathway[29]. When we treated mice with a Src inhibitor following DSS, tracing events from *Bhlha15*$^{+}$ cells was significantly inhibited by the Src inhibitor (Fig. S8J–K). Thus, for colonic regeneration following DSS treatment, the activation of Src/YAP/Wnt pathway appears to be critical.

Next, we explored whether *Bhlha15*$^{+}$ colonic precursors can give rise to tumor in the setting of *Apc* loss. The vast majority (80%) of *Bhlha15*-CreERT; *Apc*$^{flox/flox}$ mice did not develop macroscopic tumors in the colon, although on close inspection rare mice did show polypoid lesions that exhibited histologically intramucosal dysplasia (Fig. S9A). When we treated mice with DSS, we found macroscopic tumors with dysplastic histology and marked expansion of nuclear β-catenin^{+} cells in 90% of the mice (Fig. 7E–F&S9A). Addition of mutant *Kras* or *Trp53* gene expression in *Bhlha15*-CreERT; *Apc*$^{flox/flox}$ mice did not increase tumor formation (Fig. 7F). As reported previously[30], DSS treatment accelerates colonic tumor growth in *Lgr5*-CreERT; *Apc*$^{flox/flox}$ mice as well, however, histopathology of these tumors is quite similar to what was observed in DSS-treated *Bhlha15*-CreERT; *Apc*$^{flox/flox}$ mouse colon. Although DSS treatment initially activates the Wnt/YAP pathway but not the Notch pathway, all of established tumors and dysplastic lesions in both mouse lines display strong expression of YAP and HES1, without significant differences in the key Wnt/Notch target gene expression regardless of initial DSS treatment (Fig. S9B–C). These findings suggest that DSS-induced YAP/Wnt activation is responsible for initiating colonic tumors from additional cells-of-origins (e.g. progenitor cells beyond classical *Lgr5*$^{+}$ stem cells), although established tumors appear to show vastly similar histological and molecular phenotypes when identical oncogenic mutations are induced.

Abnormal Notch signaling is associated with CIN-type, left-sided colon cancers with serrated histology in human.

Finally, we investigated BHLHA15 expression and Notch status in human patient samples. Similar to mice, BHLHA15 is normally expressed in Paneth and TA progenitor cells in the small intestine, as well as in rare cells near the base in the colon (Fig. S10A). The number of

BHLHA15+ epithelial cells appears to be slightly increased in inflamed colonic glands, but almost completely lost in cancer, which may suggest that BHLHA15 or *BHLHA15* is primarily a marker of differentiated secretory lineages, and that its expression disappears when cells undergo dedifferentiation. We next analyzed whether Notch signaling is activated in human colorectal cancers using a public TCGA dataset[31]. Among 55 predefined Notch-related genes, we found the most frequent mRNA upregulation or gene amplification (36%) in the *ITCH* gene, followed by *RBPJL* (16%) and *LFNG* (10%) genes. Approximately 44 % of cancer cases showed upregulation or amplification in one of these genes or the *NOTCH1* gene (Fig. S10B). Notch-activated cancer cases are significantly associated with a chromosomal instability (CIN)-type signature[31], particularly in the left-sided colon (Table S1). Notch-activated cancers are also positively correlated with the presence of serrated features on histology (Fig. S10C&Table S1–2). On the other hand, serrated features are not significantly correlated with other oncogenic mutations, while *KRAS* or *BRAF* mutants tend to show serrated histology more frequently ($p = 0.058$ and 0.051, respectively). Cases with *RBPJL* gene alterations show significantly worse outcome compared to cases without *RBPJL* abnormalities (Fig. S10D).

Among human colorectal adenomas, HES1 expression is found in 36 % of tubular adenoma cases, and 80 % of serrated polyps, suggesting the presence of Notch activation particularly in early serrated preneoplasia (Fig. S10E–F). Given that *Itch*, *Rbpjl*, and *Lfng* genes were upregulated in Notch-activated, *Apc*-deleted mouse tumors compared to tumors with *Apc* deletion alone (Fig. S10G), Notch activation may play an important role in human colorectal serrated-type carcinogenesis.

Discussion

Recent studies have suggested a greater degree of cellular plasticity in the gastrointestinal epithelium than previously expected, and multiple cell types appear to be capable of interconverting into stem-like cells. Our data and previous studies suggest that not all progenitors can equally behave as a reserve stem cell following unspecified injurious stimuli[12–15]. Studies in the past demonstrated that *Bmi1*$^+$ cells and *Alpi*$^+$ EPs can give rise to active stem-like cells following *Lgr5*-DT ablation[11–15]. Given the absence of tracing events from *Bhlha15*$^+$ cells after *Lgr5* ablation, *Bhlha15*$^+$ precursors may play a secondary role compared to these immediate progenitors in the ISC hierarchy. Nevertheless, even the more reserved *Bhlha15*$^+$ secretory precursors are able to become reprogrammed into long-lived cancer-initiating cells, primarily in response to sustained Notch activation.

The interconversion process appears to be accompanied by dynamic genetic and epigenetic alterations in these reserve progenitors, leading to a reversion towards an *Lgr5*$^+$ cell identity[11]. In contrast, our microarray data revealed only minimal change in *Lgr5*-ablated *Bhlha15*$^+$ precursors, and thus no phenotypic interconversion in this setting. However, following irradiation and even more so after doxorubicin treatment, there are numerous gene expression changes in *Bhlha15*$^+$ precursors, although the changes did not correlate with *Lgr5*$^+$ ISC gene signature contrasting with previous reports[11]. Nonetheless, we observed short-term enterocyte-specific tracing from doxorubicin-treated *Bhlha15*$^+$ precursors. Lack of long-term lineage tracing in vivo, as well as clonogenic colony formation in vitro, suggest

that such short-term conversion may not represent true dedifferentiation and stem cell interconversion. Careful and comprehensive analysis is required to evaluate the true cellular plasticity, which may not be reflected simply by short-term tracing or temporal proliferation.

It is important to note that the expression of most reported stem and progenitor markers is not restricted to one cell types, but can be observed in a number of lineages and thus a broader heterogeneous cell population[4, 12, 15, 25]. Along these lines, we show here that *Bhlha15* expression in the intestine is not confined to mature Paneth cells, but is also detected in secretory precursors including pre-Paneth LRCs that functionally behave in a manner distinct from Paneth cells. Previous reports suggested that these *Lgr5*^{lo} pre-Paneth precursors represent slowly cycling LRCs, which do not behave as other *Lgr5*$^{+}$ CBCs but instead can dedifferentiate into active ISCs following injury[15, 24]. However, it is not entirely clear whether such LRCs are one entity, or also represent a heterogeneous population. Our comparison between *Bhlha15*$^{+}$ cells and DLL1^{+} cells suggests that secretory precursors also may be heterogeneous and contain several cell types, and that not all secretory progenitors behave in an equivalent manner, either phenotypically or genotypically. Although our data suggest that CD24^{lo} TA progenitors, rather than CD24^{hi} Paneth cell lineage, preferentially contribute to long-lived clones, it is certainly possible that both populations participate to some extent in the regeneration process, as recently reported[32, 33]. Nonetheless, our careful observations in conjunction with previous studies[15, 22] supports the notion that the ability of such interconversion or dedifferentiation is predominantly restricted to cells in undifferentiated state.

Serrated dysplasia or adenoma can be classified two main subtypes, traditional serrated adenoma (TSA) and sessile serrated adenoma (SSA). The former predominantly arises in the left-sided colon, while the latter is more frequently seen in the right-sided colon. Both adenomas are thought to be precursors of colorectal cancer, but their molecular signatures suggest that SSA-derived cancers likely represent MSI/CIMP-type accompanied with frequent *BRAF* mutation, while TSA can progress to cancers carrying classical gene mutations such as *KRAS, TP53*, or *APC* by following adenoma-carcinoma sequence[34]. However, it has not been understood how serrated histological signatures are created within these tumors. Based on our analysis, Notch signaling may contribute to serrated histology, particularly CIN-type left-sided cancers that likely include TSA-derived cancers, and our mouse model may phenocopy this particular subtype. Additionally, given that most of *Lgr5*$^{+}$ cells are ablated and *Bhlha15*$^{+}$ precursors can act as stem-like cells in the colon following injury, injury-resistant cells such as *Bhlha15*$^{+}$ progenitors or DCLK1^{+} cells[18] may be important sources of inflammation-associated colorectal cancers.

Supplementary Material

Refer to Web version on PubMed Central for supplementary material.

Acknowledgements

Authors received the NIH grants (R35CA210088 (T.C.W.) and 5U01DK103155-04 (T.C.W. & C.G.). Y.Hayakawa is supported by the KAKENHI Grant-in-Aid for Scientific Research, 17K09347 and 17H05081, P-CREATE from AMED, the Mitsubishi Foundation, Natural Sciences, the research grant of Astellas Foundation for Research on

Metabolic Disorders, the Yasuda Medical Foundation, and the Takeda Science Foundation Visionary Research Grant, the Princess Takamatsu Cancer Research Fund, and the Advanced Research and Development Programs for Medical Innovation (PRIME). R.N. is supported by the KAKENHI Grant-in-Aid for Scientific Research 17K15928.

References

1. Clevers H The intestinal crypt, a prototype stem cell compartment. Cell 2013;154:274–84. [PubMed: 23870119]
2. Middelhoff M, Westphalen CB, Hayakawa Y, et al. Dclk1-expressing tuft cells: critical modulators of the intestinal niche? Am J Physiol Gastrointest Liver Physiol 2017;313:G285–G299. [PubMed: 28684459]
3. Tian H, Biehs B, Chiu C, et al. Opposing activities of Notch and Wnt signaling regulate intestinal stem cells and gut homeostasis. Cell Rep 2015;11:33–42. [PubMed: 25818302]
4. Yan KS, Janda CY, Chang J, et al. Non-equivalence of Wnt and R-spondin ligands during Lgr5+ intestinal stem-cell self-renewal. Nature 2017;545:238–242. [PubMed: 28467820]
5. Shroyer NF, Helmrath MA, Wang VY, et al. Intestine-specific ablation of mouse atonal homolog 1 (Math1) reveals a role in cellular homeostasis. Gastroenterology 2007;132:2478–88. [PubMed: 17570220]
6. Barker N, van Es JH, Kuipers J, et al. Identification of stem cells in small intestine and colon by marker gene Lgr5. Nature 2007;449:1003–7. [PubMed: 17934449]
7. Asfaha S, Hayakawa Y, Muley A, et al. Krt19(+)/Lgr5(−) Cells Are Radioresistant Cancer-Initiating Stem Cells in the Colon and Intestine. Cell Stem Cell 2015;16:627–38. [PubMed: 26046762]
8. Sangiorgi E, Capecchi MR. Bmi1 is expressed in vivo in intestinal stem cells. Nat Genet 2008;40:915–20. [PubMed: 18536716]
9. Tian H, Biehs B, Warming S, et al. A reserve stem cell population in small intestine renders Lgr5-positive cells dispensable. Nature 2011;478:255–9. [PubMed: 21927002]
10. Metcalfe C, Kljavin NM, Ybarra R, et al. Lgr5+ stem cells are indispensable for radiation-induced intestinal regeneration. Cell Stem Cell 2014;14:149–59. [PubMed: 24332836]
11. Jadhav U, Saxena M, O'Neill NK, et al. Dynamic Reorganization of Chromatin Accessibility Signatures during Dedifferentiation of Secretory Precursors into Lgr5+ Intestinal Stem Cells. Cell Stem Cell 2017;21:65–77 e5. [PubMed: 28648363]
12. Yan KS, Gevaert O, Zheng GXY, et al. Intestinal Enteroendocrine Lineage Cells Possess Homeostatic and Injury-Inducible Stem Cell Activity. Cell Stem Cell 2017;21:78–90 e6. [PubMed: 28686870]
13. van Es JH, Sato T, van de Wetering M, et al. Dll1+ secretory progenitor cells revert to stem cells upon crypt damage. Nat Cell Biol 2012;14:1099–104. [PubMed: 23000963]
14. Tetteh PW, Basak O, Farin HF, et al. Replacement of Lost Lgr5-Positive Stem Cells through Plasticity of Their Enterocyte-Lineage Daughters. Cell Stem Cell 2016;18:203–13. [PubMed: 26831517]
15. Buczacki SJ, Zecchini HI, Nicholson AM, et al. Intestinal label-retaining cells are secretory precursors expressing Lgr5. Nature 2013;495:65–9. [PubMed: 23446353]
16. Barker N, Ridgway RA, van Es JH, et al. Crypt stem cells as the cells-of-origin of intestinal cancer. Nature 2009;457:608–11. [PubMed: 19092804]
17. Schwitalla S, Fingerle AA, Cammareri P, et al. Intestinal tumorigenesis initiated by dedifferentiation and acquisition of stem-cell-like properties. Cell 2013;152:25–38. [PubMed: 23273993]
18. Westphalen CB, Asfaha S, Hayakawa Y, et al. Long-lived intestinal tuft cells serve as colon cancer-initiating cells. J Clin Invest 2014;124:1283–95. [PubMed: 24487592]
19. Hayakawa Y, Ariyama H, Stancikova J, et al. Mist1 Expressing Gastric Stem Cells Maintain the Normal and Neoplastic Gastric Epithelium and Are Supported by a Perivascular Stem Cell Niche. Cancer Cell 2015;28:800–14. [PubMed: 26585400]
20. Hayakawa Y, Sakitani K, Konishi M, et al. Nerve Growth Factor Promotes Gastric Tumorigenesis through Aberrant Cholinergic Signaling. Cancer Cell 2017;31:21–34. [PubMed: 27989802]

21. Sakitani K, Hayakawa Y, Deng H, et al. CXCR4-expressing Mist1(+) progenitors in the gastric antrum contribute to gastric cancer development. Oncotarget 2017;8:111012–111025. [PubMed: 29340033]
22. Kinoshita H, Hayakawa Y, Niu Z, et al. Mature gastric chief cells are not required for the development of metaplasia. Am J Physiol Gastrointest Liver Physiol 2018.
23. Hayakawa Y, Hirata Y, Nakagawa H, et al. Apoptosis signal-regulating kinase 1 regulates colitis and colitis-associated tumorigenesis by the innate immune responses. Gastroenterology 2010;138:1055–67.e1–4. [PubMed: 19931259]
24. Barriga FM, Montagni E, Mana M, et al. Mex3a Marks a Slowly Dividing Subpopulation of Lgr5+ Intestinal Stem Cells. Cell Stem Cell 2017;20:801–816 e7. [PubMed: 28285904]
25. Grun D, Lyubimova A, Kester L, et al. Single-cell messenger RNA sequencing reveals rare intestinal cell types. Nature 2015;525:251–5. [PubMed: 26287467]
26. Haber AL, Biton M, Rogel N, et al. A single-cell survey of the small intestinal epithelium. Nature 2017;551:333–339. [PubMed: 29144463]
27. Rothenberg ME, Nusse Y, Kalisky T, et al. Identification of a cKit(+) colonic crypt base secretory cell that supports Lgr5(+) stem cells in mice. Gastroenterology 2012;142:1195–1205 e6. [PubMed: 22333952]
28. Sasaki N, Sachs N, Wiebrands K, et al. Reg4+ deep crypt secretory cells function as epithelial niche for Lgr5+ stem cells in colon. Proc Natl Acad Sci U S A 2016;113:E5399–407. [PubMed: 27573849]
29. Yui S, Azzolin L, Maimets M, et al. YAP/TAZ-Dependent Reprogramming of Colonic Epithelium Links ECM Remodeling to Tissue Regeneration. Cell Stem Cell 2018;22:35–49 e7. [PubMed: 29249464]
30. Tauriello DVF, Palomo-Ponce S, Stork D, et al. TGFbeta drives immune evasion in genetically reconstituted colon cancer metastasis. Nature 2018;554:538–543. [PubMed: 29443964]
31. Cancer Genome Atlas N Comprehensive molecular characterization of human colon and rectal cancer. Nature 2012;487:330–7. [PubMed: 22810696]
32. Yu S, Tong K, Zhao Y, et al. Paneth Cell Multipotency Induced by Notch Activation following Injury. Cell Stem Cell 2018;23:46–59 e5. [PubMed: 29887318]
33. Schmitt M, Schewe M, Sacchetti A, et al. Paneth Cells Respond to Inflammation and Contribute to Tissue Regeneration by Acquiring Stem-like Features through SCF/c-Kit Signaling. Cell Rep 2018;24:2312–2328 e7. [PubMed: 30157426]
34. JE IJ, Vermeulen L, Meijer GA, et al. Serrated neoplasia-role in colorectal carcinogenesis and clinical implications. Nat Rev Gastroenterol Hepatol 2015;12:401–9. [PubMed: 25963511]

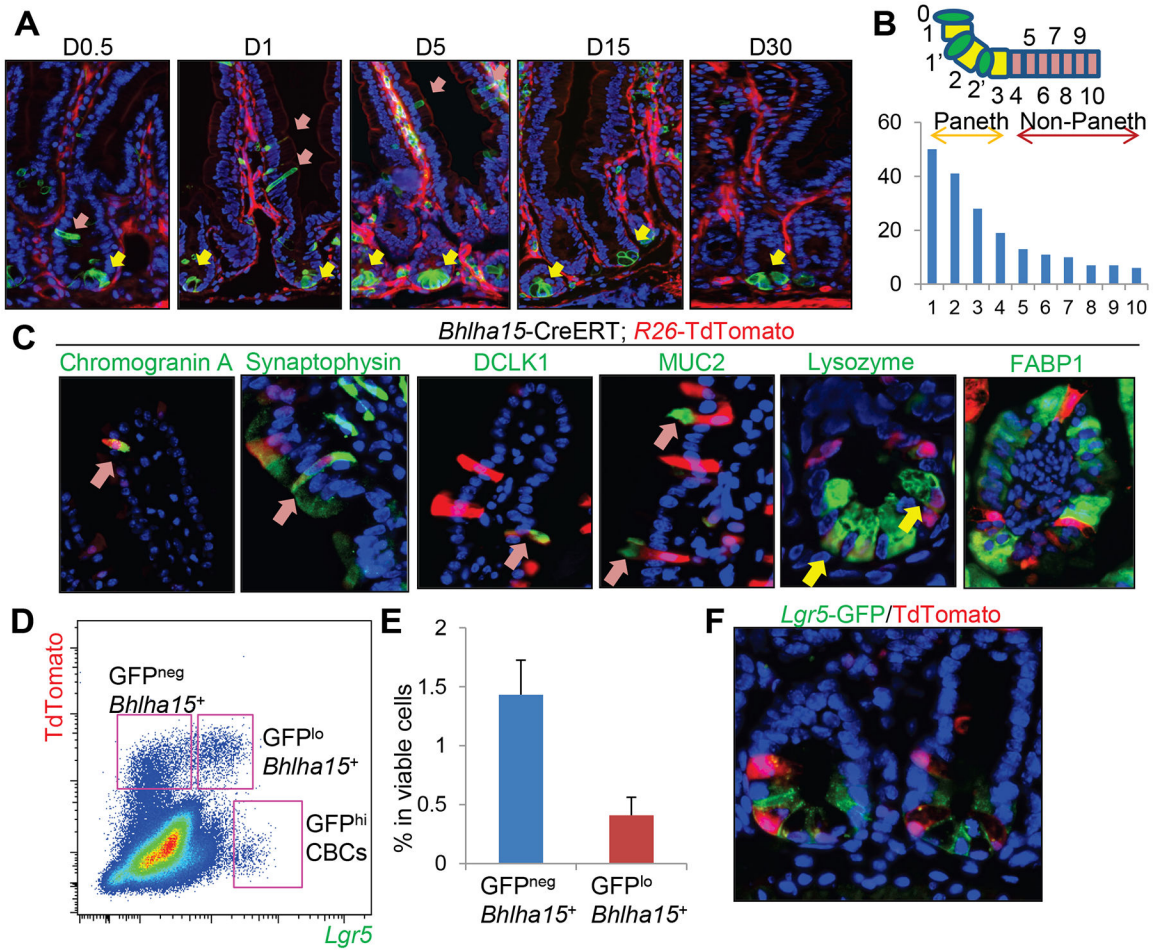

Figure 1. *Bhlha15* is expressed in the short-lived secretory precursors.

(A)Lineage tracing in *Bhlha15*-CreERT;*R26*-mTmG small intestine at indicated time points after tamoxifen. Yellow allows; Paneth cells, pink arrows; non-Paneth cells. (B)Cell position of *Bhlha15*$^{+}$ cells in jejunum. Total 60 crypts from 3 mice were quantified. (C)Immunostaining in *Bhlha15*-CreERT;*R26*-TdTomato mice 5 days after tamoxifen. Arrows indicate double-positive cells. (D-F)FACS plot (D), percentage of indicated populations in viable cells (E, n=3), and image (F) of *Bhlha15*-CreERT;*Lgr5*-DTR-EGFP;*R26*-TdTomato mouse intestine 12 hours after tamoxifen. Mean±S.E.M.

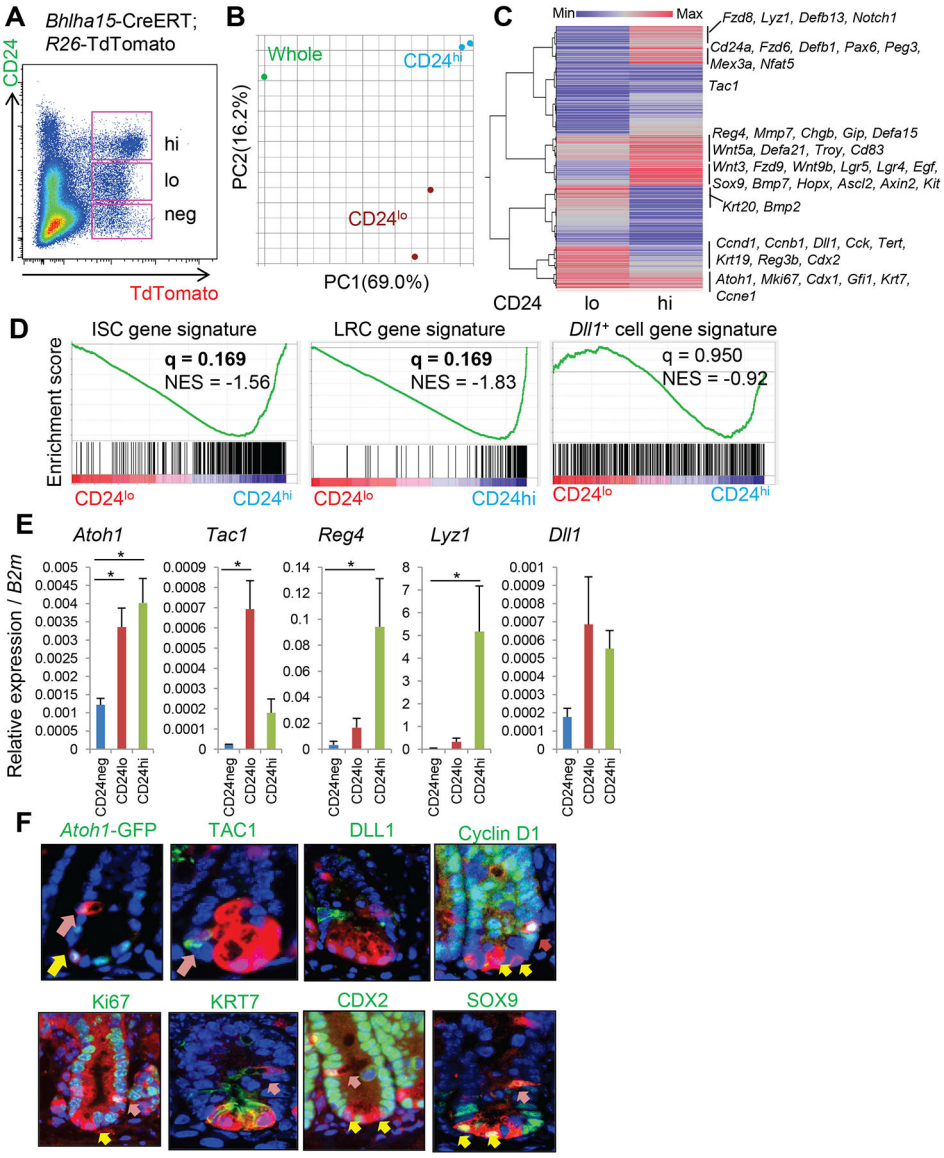

Figure 2. Transcriptome analysis of *Bhlha15*-expressing populations.

(A)FACS analysis of *Bhlha15*-CreERT;*R26*-TdTomato mouse intestine 2 days after tamoxifen with CD24 immunostaining. Pink boxes indicate CD24^{neg}, CD24^{lo}, and CD24^{hi} population among TdTomato^{+} cells. (B)PCA analysis of gene expression in TdTomato $^{+}$CD24^{lo}, TdTomato^{+}CD24^{hi} cells, and whole intestine. (C)Hierarchical clustering of average gene expression in TdTomato^{+}CD24^{lo} and TdTomato^{+}CD24^{hi} cells compared to whole intestine. (D)GSEA analysis for the comparison between TdTomato^{+}CD24^{lo} and TdTomato^{+}CD24^{hi} cells. (E)RT-PCR of sorted TdTomato^{+}CD24^{neg}, TdTomato^{+}CD24^{lo}, and TdTomato^{+}CD24^{hi} population (n=4). (F)Staining (green) in *Bhlha15*-CreERT;*R26*-TdTomato mice 1 day after tamoxifen. Yellow arrows; Paneth cells, pink arrows; non-Paneth secretory cells. Mean±S.E.M. *p<0.05.

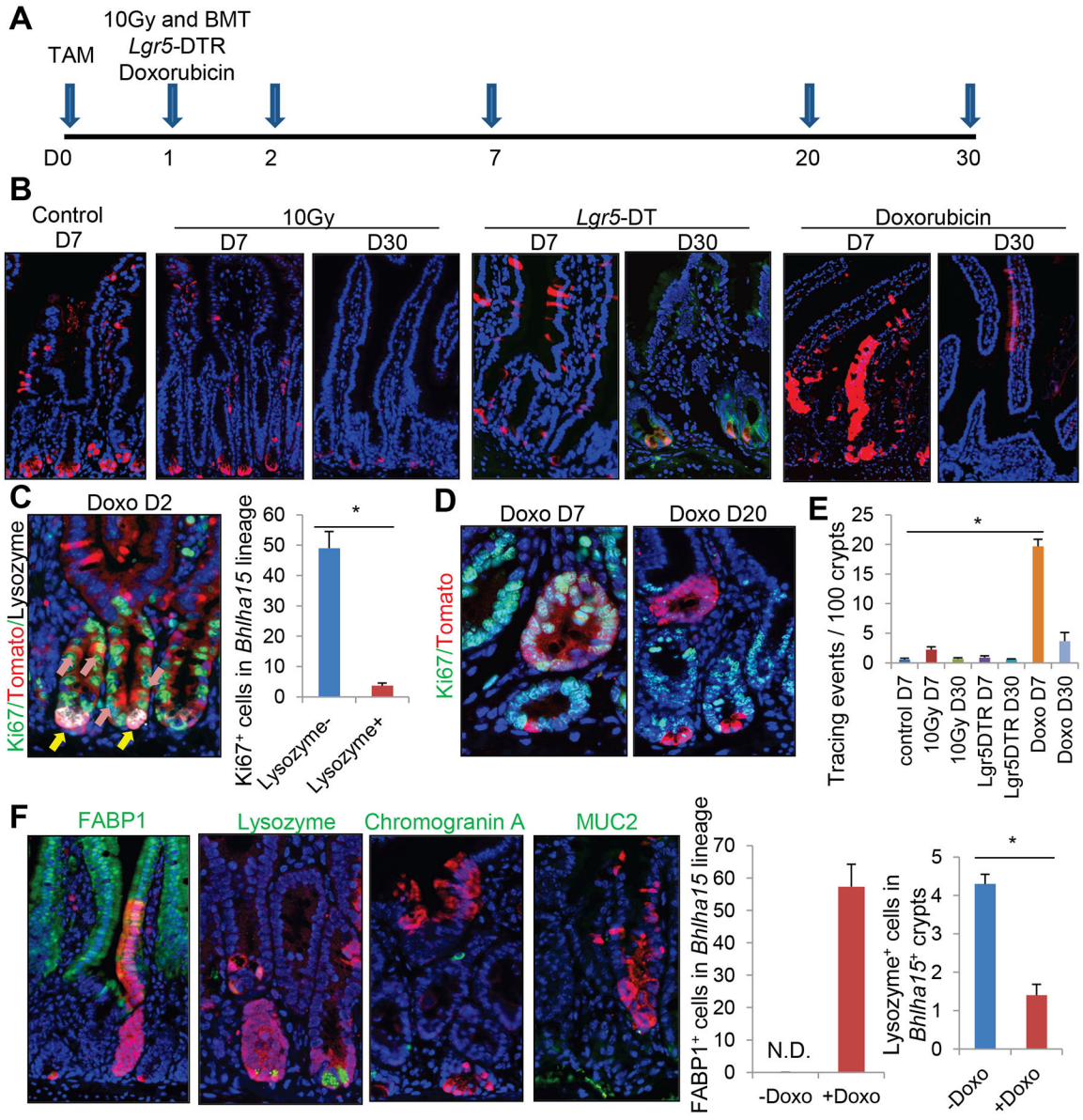

Figure 3. *Bhlha15*$^{+}$ precursors show short-term lineage tracing following doxorubicin-induced injury, but do not convert to long-lived ISCs.

(A)Protocol. (B)Lineage tracing images of *Bhlha15*-CreERT;*R26*-TdTomato mouse intestine after 10-Gy whole body irradiation, *Lgr5*-DT ablation, or doxorubicin. WT bone marrow was transplanted after irradiation. (C)Ki67 (green), RFP (red), and Lysozyme (gray) staining on doxorubicin-treated *Bhlha15*-CreERT;*R26*-TdTomato mouse at day 2. Numbers of Ki67^{+} cells in 100 Tomato^{+}Lysozyme^{+} or Lysozyme^{-} cells are quantified. n=3/group. (D)Ki67 (green) and RFP (red) staining on doxorubicin-treated *Bhlha15*-CreERT;*R26*-TdTomato mice. (E)Lineage tracing events per 100 glands in *Bhlha15*-CreERT mouse intestine. n=3/group. (F)Immunostaining (green) of TdTomato-expressing clones in *Bhlha15*-CreERT;*R26*-TdTomato mice 7 days after doxorubicin. Numbers of FABP1^{+} and Lysozyme^{+} cells in 100 Tomato^{+} cells are quantified. n=3/group. Mean±S.E.M. *p<0.05.

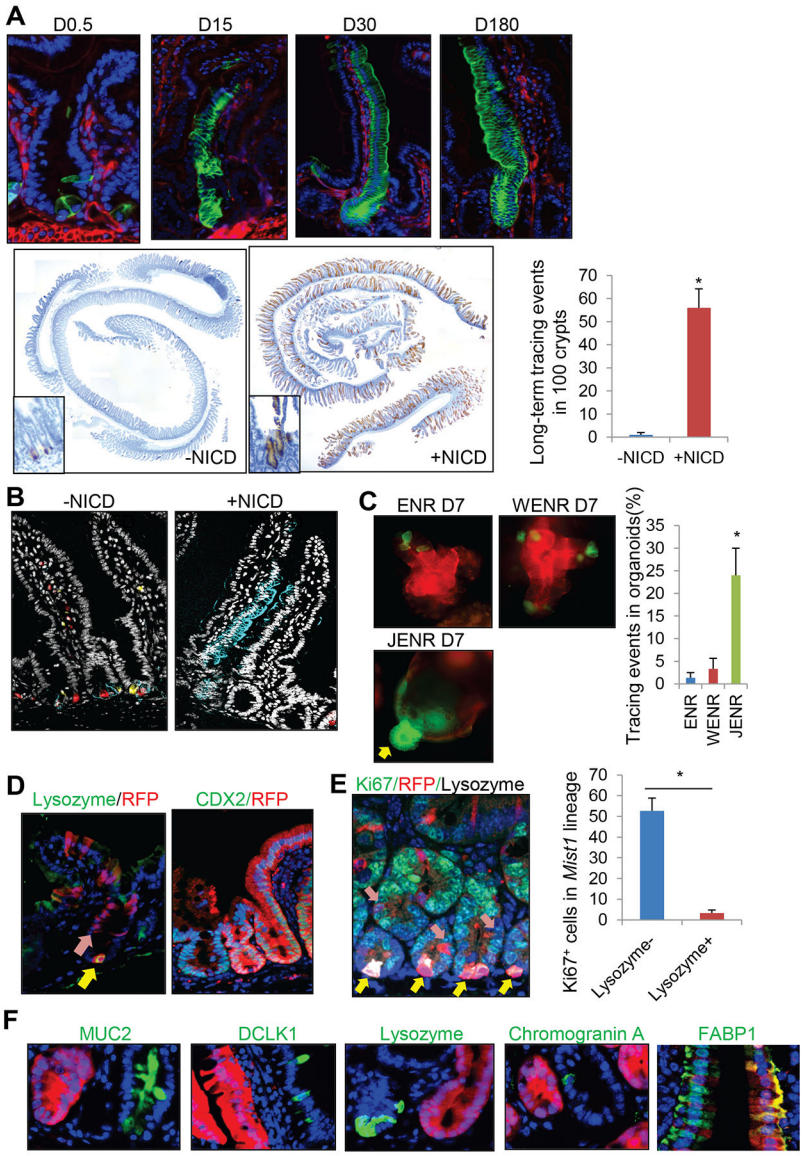

Figure 4. *Bhlha15*$^{+}$ precursors show long-term enterocyte-specific lineage tracing with sustained Notch activation.

(A)Lineage tracing images of *Bhlha15*-CreERT;LSL-Notch1(IC);*R26*-mTmG (top) and RFP staining and quantification of *Bhlha15*-CreERT;*R26*-TdTomato and *Bhlha15*-CreERT;LSL-Notch1(IC);*R26*-TdTomato mouse intestine. Tracing events per 100 glands were quantified at 180 days after tamoxifen (n=3). (B)*Bhlha15*-CreERT;*R26*-Confetti and *Bhlha15*-CreERT;LSL-Notch1(IC);*R26*-Confetti mouse intestines 14 days after tamoxifen. (C)Organoid culture of *Bhlha15*-CreERT;*R26*-mTmG mouse intestine. Tamoxifen was given at day 0, and glands were taken after 12 hours. Crypts were cultured with indicated medium for 7 days, and tracing events ratio in total organoids were quantified (n=3). (D)Lysozyme (day5) and CDX2 staining (day30) on *Bhlha15*-CreERT;LSL-Notch1(IC);*R26*-TdTomato mice. (E)Ki67 (green), RFP (red), and Lysozyme (gray) staining 4 days after tamoxifen. Numbers of Ki67^{+} cells in 100 Tomato^{+}Lysozyme^{+} or Lysozyme^{-} cells are quantified. n=3/

group. (F)Immunostaining (green) in *Bhlha15*-CreERT;LSL-Notch1(IC);*R26*-TdTomato mice. Mean±S.E.M. *p<0.05.

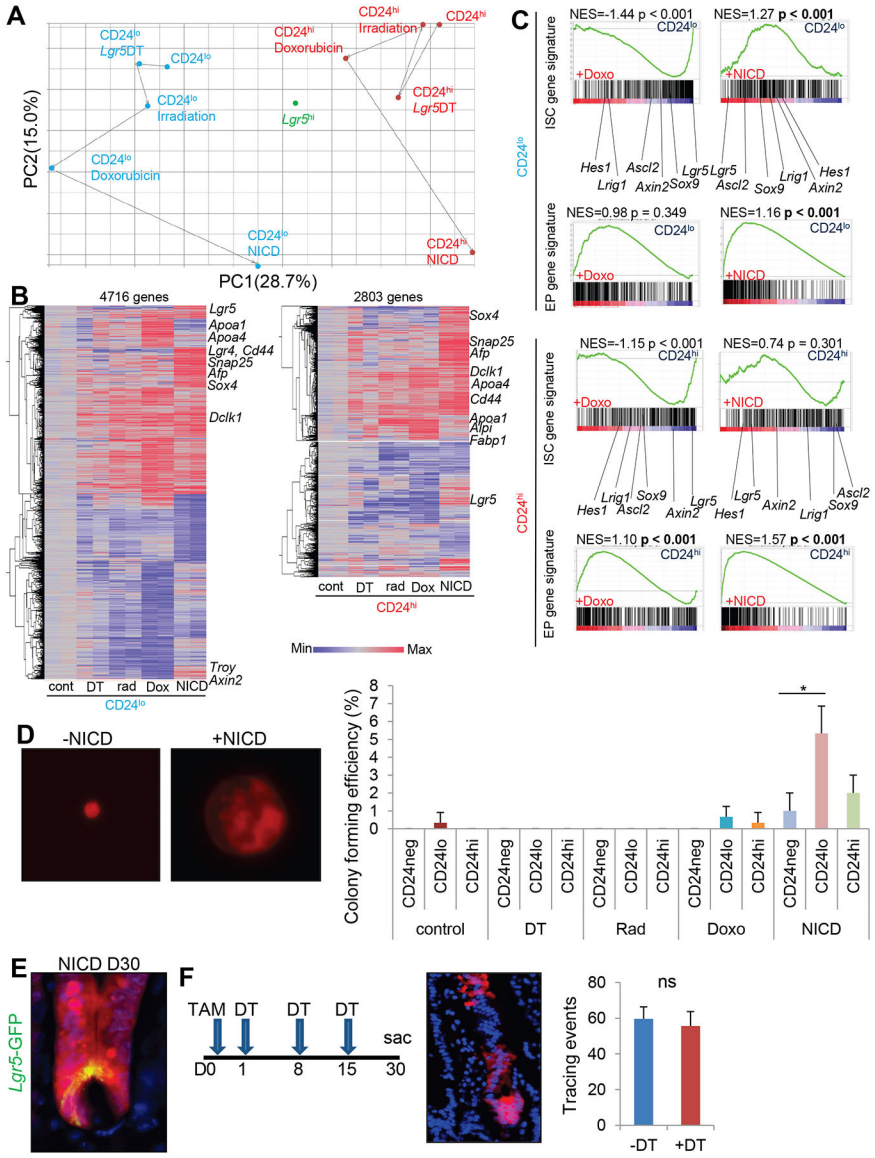

Figure 5. Distinct gene profiles in activated *Bhlha15*$^{+}$ cells.

(A)PCA analysis of average gene expression (n=2/group) in TdTomato^{+}CD24^{lo}, TdTomato^{+}CD24^{hi}, and *Lgr5*^{hi} cells after treatment. (B)Hierarchical clustering of gene expression in the individual TdTomato^{+}CD24^{lo} and TdTomato^{+}CD24^{hi} cells compared to the untreated cells. (C)GSEA analysis for the indicated comparison between untreated TdTomato^{+}CD24^{lo} or CD24^{hi} cells and cells after doxorubicin or NICD expression. (D)Representative single cell culture images and colony forming efficiency of each population. Cells were sorted and collected from 3 mice/group, and 1000 singlet cells per well were cultured (3 wells/group). Colony formation rate at day 10 is shown. (E)*Bhlha15*-CreERT;LSL-Notch1(IC);*Lgr5*-DTR-EGFP;*R26*-TdTomato intestines 30 days after tamoxifen. (F)*Bhlha15*-CreERT;LSL-Notch1(IC);*Lgr5*-DTR-EGFP;*R26*-TdTomato intestines 30 days after tamoxifen and DT treatment. Tracing events per 100 glands were quantified. n=3/group. Mean±S.E.M. *p<0.05.

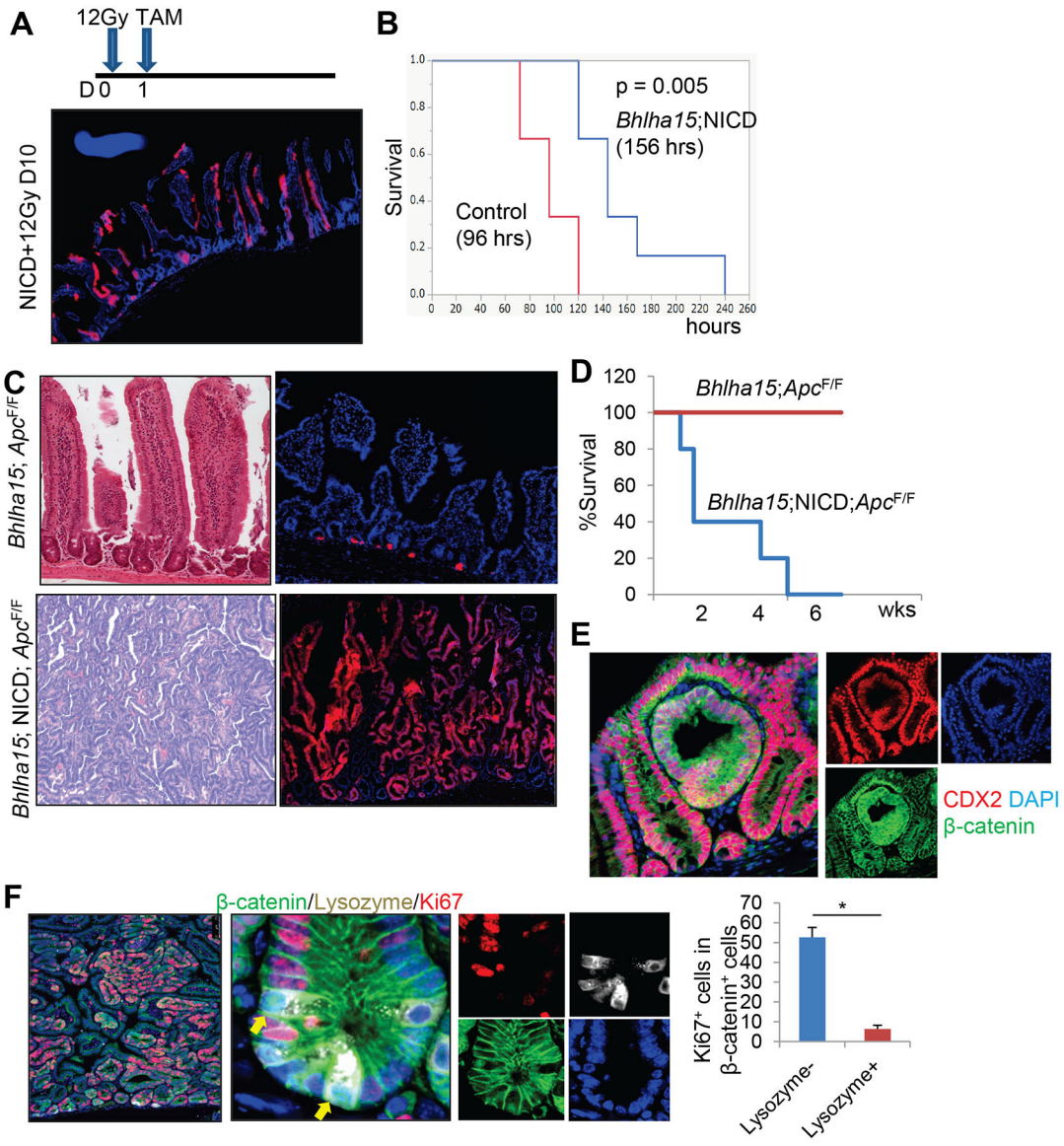

Figure 6. NICD^{+}*Bhlha15*$^{+}$ progenitors contribute to regeneration and cancer.

(A)*Bhlha15*-CreERT;LSL-Notch1(IC);*R26*-TdTomato mice were irradiated at the dose of 12Gy and given tamoxifen at day 1. (B)Survival rate of 12Gy-irradiated *Bhlha15*-CreERT;*R26*-TdTomato (n=6) and *Bhlha15*-CreERT;LSL-Notch1(IC); *R26*-TdTomato mice (n=5). (C)H&E and TdTomato expression of *Bhlha15*-CreERT;*Apc*$^{flox/flox}$;*R26*-TdTomato and *Bhlha15*-CreERT;LSL-Notch1(IC);*Apc*$^{flox/flox}$;*R26*-TdTomato mouse intestine at day 20. (D)Survival curve of *Bhlha15*-CreERT;*Apc*$^{flox/flox}$ (red) and *Bhlha15*-CreERT;LSL-Notch1(IC);*Apc*$^{flox/flox}$ (blue) mice. (E-F)CDX2 (red) and β-catenin (green) staining (E) and Ki67 (red), Lysozyme (gray), and β-catenin (green) staining (F) of *Bhlha15*-CreERT;LSL-Notch1(IC);*Apc*$^{flox/flox}$ mice at day 10. Numbers of Ki67^{+} cells in 100 β-catenin^{+}Lysozyme^{+} or β-catenin^{+}Lysozyme^{-} cells are quantified (n=3). Mean±S.E.M. *p<0.05.

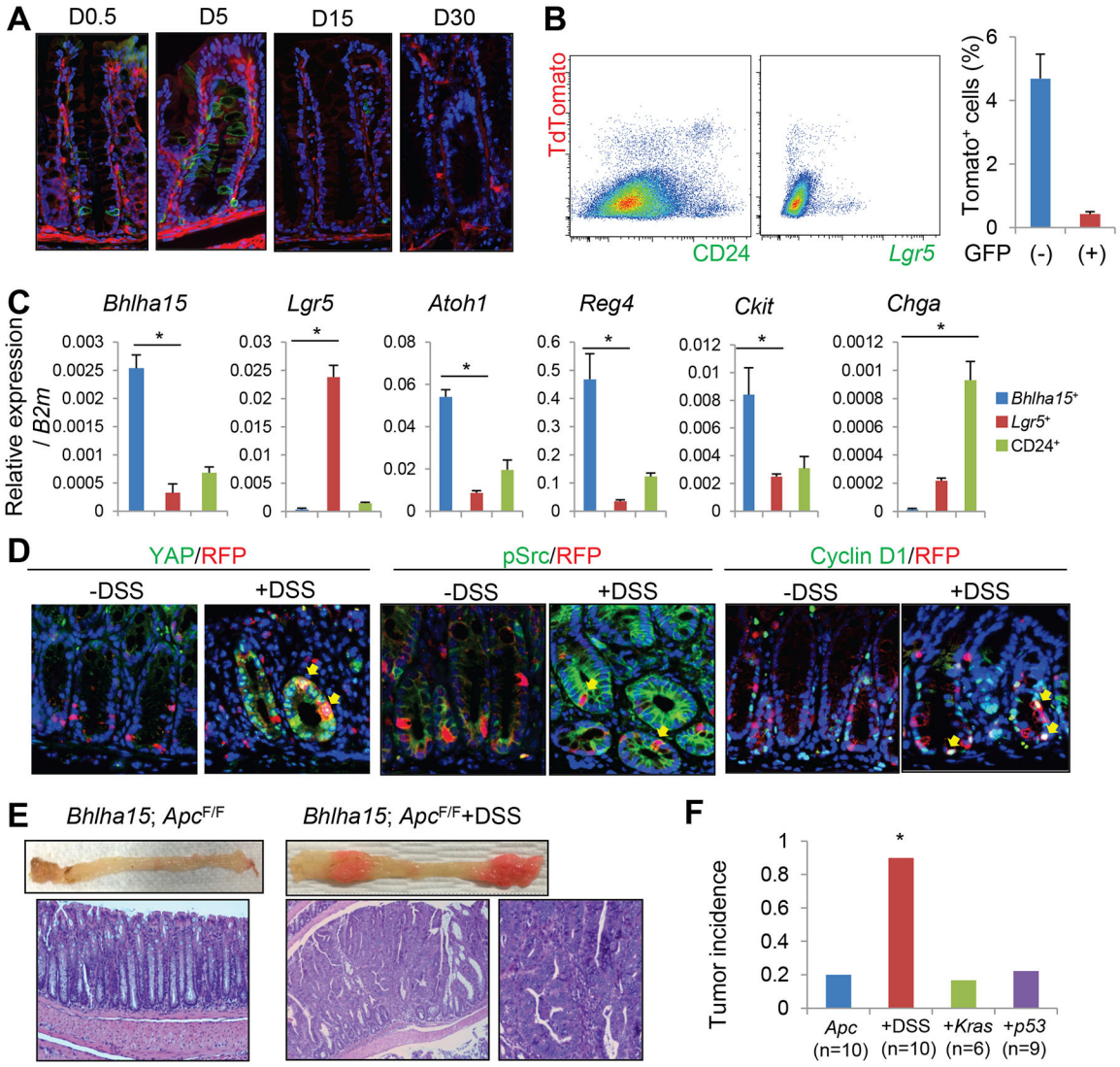

Figure 7. *Bhlha15* marks colonic secretary precursors that can lineage trace following injury.

(A)Lineage tracing of *Bhlha15*-CreERT;*R26*-mTmG mouse colon. (B)FACS analysis of *Bhlha15*-CreERT;*Lgr5*-DTR-EGFP;*R26*-TdTomato mouse colon 1 day after tamoxifen, gated by CD24 (left) or GFP (right). Percentages of $GFP^{+}Tomato^{+}$ and $GFP^{-}Tomato^{+}$ cells in viable cells are shown (n=3). (C)RT-PCR analysis of sorted $TdTomato^{+}CD24^{+}$, $TdTomato^{-}CD24^{+}$, and *Lgr5*-GFP^{+} cells (n=3). (D)YAP, pSrc, and cyclin D1 staining (green) of *Bhlha15*-CreERT;*R26*-TdTomato mouse colon with or without DSS. Tamoxifen was given 1 day after DSS treatment, then mice were analyzed on next day. (E)Macroscopic images and H&E staining of *Bhlha15*-CreERT;$Apc^{flox/flox}$ mouse colon with or without DSS treatment. (F)Colon tumor incidence in *Bhlha15*-CreERT;$Apc^{flox/flox}$ mice with DSS treatment, LSL-$Kras^{G12D}$, or LSL-$Trp53^{R172H}$. Mean±S.E.M. *p<0.05.